C2

NATIONAL ADVISORY COMMITTEE

FOR AERONAUTICS

TECHNICAL NOTE 3958

ANALYSIS OF STATIC AEROELASTIC BEHAVIOR

OF LOW-ASPECT-RATIO RECTANGULAR WINGS

By John M. Hedgepeth and Paul G. Waner, Jr.

Langley Aeronautical Laboratory
Langley Field, Va.

NACA

Washington

April 1957

ANALYSIS OF STATIC AEROELASTIC BEHAVIOR

OF LOW-ASPECT-RATIO RECTANGULAR WINGS

By John M. Hedgepeth and Paul G. Waner, Jr.

SUMMARY

Slender-body theory is used in conjunction with plate theory to analyze the static aeroelastic-divergence behavior of low-aspect-ratio rectangular wings of constant thickness when chordwise deformations are considered. In the analysis, the spanwise variation of the deflection is restricted to a parabola but the chordwise variation is allowed complete freedom. Results show the variation of the divergence speed and mode shape with the aspect ratio. Comparisons are made with results obtained by using approximate (linear, parabolic, and cubic) chordwise deflection shapes.

INTRODUCTION

Methods for predicting the divergence speed of wings when chordwise deformations are neglected have been treated extensively in the past. For wings with fairly large aspect ratios, accurate results have been obtained; however, for wings with low aspect ratios, the chordwise deformations can no longer be neglected.

A number of analyses are available that deal with the effects of chordwise deformation on divergence. Among them are the works of Miles (ref. 1) and Biot (ref. 2). Miles considered the chordwise divergence of a delta wing cantilevered along its trailing edge. He assumed that the deformations of the wing were cylindrical with straight-line generators in the spanwise direction. Biot, on the other hand, considered an unswept wing and included both spanwise and chordwise structural effects. In Biot's work, the use of aerodynamic strip theory limits the value of his analysis for low-aspect-ratio wings.

In the present paper an analysis is made of the divergence of very low-aspect-ratio cantilever plates of uniform thickness (see fig. 1). Allowance has been made for the presence of additional discrete chordwise stiffening elements. Although the analysis includes both spanwise and chordwise structural effects, primary emphasis is placed on the chordwise

deformations. Indeed, the primary purposes of this study are to determine the types of chordwise deflection shapes which can be expected in very low-aspect-ratio wings and to assess the accuracy resulting from the use of approximate chordwise mode shapes in aeroelastic analyses.

Slender-body theory (see ref. 3, for example) is used to determine the aerodynamic loads, and plate theory is used in conjunction with a potential-energy approach to determine the deformations. Numerical results are presented for wings with various aspect ratios and chordwise stiffnesses.

SYMBOLS

A	aspect ratio
a_1, a_2, a_3	coefficients defined by equations (17)
c	wing chord
D	plate stiffness in bending, $Et^3/12\left(1 - \mu^2\right)$
E	Young's modulus of elasticity
$(EI)_e$	total effective bending stiffness of chordwise stiffeners (See eq. (19).)
$(EI)_i$	bending stiffness of ith stiffener
$f(x)$, $f(\xi)$	chordwise deflection shape
N	total number of chordwise stiffeners
$P_1(x)$	generalized aerodynamic loading (See eq. (13).)
$p(x,y)$	lift per unit area, positive in z-direction
q	dynamic pressure, $\dfrac{\rho U^2}{2}$
R	coefficient defined by equation (18)
s	wing semispan

t   wing thickness

U   free-stream velocity

V_1 generalized aerodynamic leading-edge shear (See eq. (13).)

$V(y)$ leading-edge shear

$w(x,y)$ wing deflection, positive in z-direction

x,y,z   coordinate system (See fig. 1.)

$\alpha,\beta,\bar{\beta}$ parameters defined by equations (20) and (23)

λ divergence-speed parameter, $\dfrac{5\pi}{48}\dfrac{qs^3}{D}$

μ Poisson's ratio

ξ,η nondimensional coordinates x/s, y/s, respectively

Π total potential energy of the system

σ dummy variable of integration for y

ρ free-stream density of fluid

$\phi(x,y,z)$ perturbation velocity potential

Subscript:

i   integer denoting stiffener number (See fig. 1.)

ANALYSIS

The wing configuration considered herein consists of a rectangular plate of constant thickness with a number of constant-stiffness beams in the chordwise direction (fig. 1). The wing is assumed to be supported along its center line and only symmetrical deflections are considered.

The analysis is based on the assumption that the aspect ratio of the wing is very low. For such a wing, the deflections will generally vary in a much more complicated manner in the chordwise (x) direction than in the spanwise (y) direction. It therefore seems reasonable to assume a simple spanwise variation for deflection and allow the chordwise

variation to be arbitrary. Since the simplest type of spanwise defor-
mation compatible with the support boundary conditions is a parabola,
the following assumed deflection shape is used in the analysis:

$$w(x,y) = y^2 f(x) \tag{1}$$

where $f(x)$ is the chordwise deflection shape.

The assumption of low aspect ratio also implies that Jones' slender
body theory (ref. 3), in which streamwise perturbations are considered
negligible in comparison with perturbations in the crossflow directions,
can be used to determine the aerodynamic loading caused by the deforma-
tion of equation (1). Although slender-body theory is exact only in the
limit $\left(1 - M^2\right)A^2 \to 0$, it is employed herein because of its ease of
application; the use of slender-body theory leads to a particularly sim-
ple formulation of the divergence problem and, hence, allows a detailed
investigation of the divergence behavior of very low-aspect-ratio wings.

In order to determine the deformations resulting from aerodynamic
loads, plate theory is employed. The principle of minimum potential
energy is used to derive the differential equation of equilibrium for
the function $f(x)$. In applying this principle, the difficulties arising
from the presence of nonconservative forces are circumvented by treating
the loads as fixed quantities during the variation. The aerodynamic loads
are then substituted into the differential equation and the solution is
obtained.

Aerodynamic Forces

For slender-body theory, the velocity-potential equation for line-
arized flow reduces to Laplace's equation in the crossflow plane:

$$\frac{\partial^2 \phi}{\partial y^2} + \frac{\partial^2 \phi}{\partial z^2} = 0 \tag{2}$$

The boundary conditions are

$$\frac{\partial \phi}{\partial z}(x,y,0) = Uy^2 \frac{df}{dx} \tag{3}$$

on the wing and $\phi = 0$ at the tips. Furthermore, derivatives of the
potential at infinity must be zero.

It is desired to calculate the potential ϕ and hence the pressure distribution resulting from the given deformation shape.

In order for equation (2) to be satisfied, with the boundary condition that $\phi = 0$ at the tips, the following relationship between $\frac{\partial\phi}{\partial y}$ (x,y,+0) (the limit of $\partial\phi/\partial y$ as z approaches zero from above) and $\frac{\partial\phi}{\partial z}$ (x,y,0) must exist (ref. 4):

$$\frac{\partial\phi(x,y,+0)}{\partial y} = \frac{1}{\pi\sqrt{s^2 - y^2}}\int_{-s}^{s} \frac{\sqrt{s^2 - \sigma^2}}{y - \sigma}\frac{\partial\phi(x,\sigma,0)}{\partial z}\,d\sigma \qquad (4)$$

Substituting $\frac{\partial\phi}{\partial z}$ (x,y,0) from equation (3) and integrating gives

$$\phi(x,y,+0) = -\frac{U}{3}f'(x)\left(\frac{s^2}{2} + y^2\right)\sqrt{s^2 - y^2} \qquad (5)$$

where the prime denotes differentiation with respect to x.

The lift per unit area of a thin wing in terms of the velocity potential is

$$p(x,y) = 2\rho U\frac{\partial\phi(x,y,+0)}{\partial x}$$

Thus, the lift per unit area is, by substitution from equation (5),

$$p(x,y) = -\frac{4}{3}qf''(x)\left(\frac{s^2}{2} + y^2\right)\sqrt{s^2 - y^2} \qquad (6)$$

In addition to the distributed pressures acting on the wing, there is a concentrated load acting along the leading edge. This concentrated load arises as a result of the application of the slender-body theory to the rectangular plan form; that is, the velocity potential is zero ahead of the leading edge and then jumps to a finite value at the leading edge. The magnitude of the resulting concentrated load is

$$V(y) = 2\rho U\phi(0,y,+0)$$

which gives, by use of equation (5),

$$V(y) = -\frac{4}{3} qf'(0)\left(\frac{s^2}{2} + y^2\right)\sqrt{s^2 - y^2} \qquad (7)$$

Structural Equilibrium

The total potential energy of the system under consideration consists of the strain energy of the wing plus the potential energy of the aerodynamic forces. The strain energy of the wing is made up of the strain energy of the plate (ref. 5)

$$\frac{D}{2}\int_0^c \int_0^s \left[\left(\frac{\partial^2 w}{\partial x^2}\right)^2 + \left(\frac{\partial^2 w}{\partial y^2}\right)^2 + 2\mu \frac{\partial^2 w}{\partial x^2}\frac{\partial^2 w}{\partial y^2} + 2(1 - \mu)\left(\frac{\partial^2 w}{\partial x \partial y}\right)^2\right] dy\ dx$$

and the energy of bending of the chordwise stiffeners (N in number)

$$\frac{1}{2}\sum_{i=1}^{N} (EI)_i \int_0^c \left[\frac{\partial^2 w(x,y_i)}{\partial x^2}\right]^2 dx$$

In these expressions, D is the plate stiffness $\left(Et^3/12\left(1 - \mu^2\right)\right)$, $(EI)_i$ is the bending stiffness of the ith stiffener, and y_i is the spanwise coordinate of the ith stiffener. (Note that because of symmetry, only half of the wing is considered.)

The foregoing analysis of the aerodynamic forces has indicated that the wing loads are composed of two parts, a distributed lift $p(x,y)$ and a concentrated load $V(y)$ located at the leading edge. The potential energy of the lift per unit area is

$$-\int_0^c \int_0^s p(x,y)w(x,y)dy\ dx$$

and the potential energy of the concentrated load is

$$-\int_0^s V(y)w(0,y)dy$$

The total potential energy of the system is the sum of these different energies, or

$$
\Pi = \frac{D}{2} \int_0^c \int_0^s \left[\left(\frac{\partial^2 w}{\partial x^2}\right)^2 + \left(\frac{\partial^2 w}{\partial y^2}\right)^2 + 2\mu \frac{\partial^2 w}{\partial x^2}\frac{\partial^2 w}{\partial y^2} + 2(1-\mu)\left(\frac{\partial^2 w}{\partial x \partial y}\right)^2 \right] dy\ dx +
$$

$$
\frac{1}{2}\sum_{i=1}^{N}(EI)_i \int_0^c \left[\frac{\partial^2 w(x,y_i)}{\partial x^2}\right]^2 dx - \int_0^c \int_0^s p(x,y)w(x,y)dy\ dx -
$$

$$
\int_0^s V(y)w(0,y)dy \tag{8}
$$

Substitution of the expression for $w(x,y)$ given by equation (1) into equation (8) results in the following expression for the total potential energy:

$$
\Pi = \frac{D}{2}\int_0^c \left\{ \left[\frac{s^5}{5} + \frac{1}{D}\sum_{i=1}^N (EI)_i y_i^4\right] f''^2 + 4sf^2 + \frac{4}{3}s^3\mu ff'' + \right.
$$

$$
\left. \frac{8}{3}s^3(1-\mu)f'^2 \right\} dx - \int_0^c P_1(x)f\ dx - V_1 f(0) \tag{9}
$$

where

$$
P_1(x) = \int_0^s p(x,y)y^2 dy
$$

$$
V_1 = \int_0^s V(y)y^2 dy
$$

$$\tag{10}$$

Minimization of the potential-energy expression by means of the calculus of variations gives

$$\delta\Pi = 0$$

$$= \frac{D}{2}\int_0^c \left\{ \left[\frac{s^5}{5} + \frac{1}{D}\sum_{i=1}^{N} (EI)_i y_i^4 \right] \delta f''^2 + 4s\delta f^2 + \frac{4}{3}s^3\mu\delta(ff'') + \right.$$

$$\left. \frac{8}{3}s^3(1 - \mu)\delta f'^2 \right\} dx - \int_0^c P_1(x)\delta f\, dx - V_1\delta f(0)$$

Integrating by parts and collecting terms results in the differential equation

$$\left[\frac{s^5}{5} + \frac{1}{D}\sum_{i=1}^{N} (EI)_i y_i^4 \right] f^{IV} + \frac{(12\mu - 8)}{3}s^3 f'' + 4sf = \frac{P_1(x)}{D} \qquad (11)$$

and the following boundary conditions:

At both $x = 0$ and $x = c$,

$$\left[\frac{s^5}{5} + \frac{1}{D}\sum_{i=1}^{N} (EI)_i y_i^4 \right] f'' + \frac{2}{3}s^3\mu f = 0 \qquad (12a)$$

At $x = 0$,

$$\left[\frac{s^5}{5} + \frac{1}{D}\sum_{i=1}^{N} (EI)_i y_i^4 \right] f''' - \frac{(8 - 10\mu)}{3}s^3 f' - \frac{V_1}{D} = 0 \qquad (12b)$$

At $x = c$,

$$\left[\frac{s^5}{5} + \frac{1}{D}\sum_{i=1}^{N}(EI)_i y_i{}^4\right]f''' - \frac{(8 - 10\mu)}{3}s^3 f' = 0 \qquad (12c)$$

Aeroelastic Solution

The differential equation and boundary conditions which describe the deflection of the structure due to the generalized aerodynamic loads $P_1(x)$ and V_1 are given by equations (11) and (12). The values of the generalized loads can be obtained by substituting $p(x,y)$ and $V(y)$ (eqs. (6) and (7)) into equations (10). This substitution gives

$$\left.\begin{aligned}P_1(x) &= -\frac{\pi}{12}s^6 q f''(x)\\[2em]V_1 &= -\frac{\pi}{12}s^6 q f'(0)\end{aligned}\right\} \qquad (13)$$

If these values of $P_1(x)$ and V_1 are substituted into the differential equation (11) and the four boundary conditions (eqs. (12)), and the equations are nondimensionalized by letting

$$\xi = \frac{x}{s}$$

and

$$\eta_i = \frac{y_i}{s}$$

the differential equation becomes

$$f^{IV}(\xi) + \frac{4}{R}\left(\lambda - a_1\right)f''(\xi) + \frac{20}{R}f(\xi) = 0$$

The four boundary conditions become:

At $\xi = 0$ or $\frac{c}{s}$,

$$f''(\xi) + \frac{a_2}{R} f(\xi) = 0$$

At $\xi = 0$,

$$f'''(\xi) + \left[\frac{4}{R}\left(\lambda - a_1\right) - \frac{a_2}{R}\right]f'(\xi) = 0$$

At $\xi = \frac{c}{s}$,

$$f'''(\xi) - \frac{4}{R} a_3 f'(\xi) = 0$$

$$(15)$$

where

$$\lambda = \frac{5\pi}{48} \frac{qs^3}{D} \qquad (16)$$

and

$$a_1 = \frac{10}{3}\left(1 - \frac{3\mu}{2}\right)$$

$$a_2 = \frac{10\mu}{3}$$

$$a_3 = \frac{10}{3}\left(1 - \frac{5\mu}{4}\right)$$

$$(17)$$

$$R = 1 + \frac{5(EI)_e}{sD} \qquad (18)$$

In equation (18), $(EI)_e$ is the total effective bending stiffness of the chordwise stiffeners and is defined as

$$(EI)_e = \sum_{i=1}^{N} (EI)_i \eta_i^4 \qquad (19)$$

The characteristic roots of the differential equation are

$$\pm \sqrt{\frac{2}{R}} \sqrt{-(\lambda - a_1) \pm \sqrt{(\lambda - a_1)^2 - 5R}}$$

The roots can be seen to be dependent on the value of $(\lambda - a_1)$. For $(\lambda - a_1)^2 > 5R$, all the roots are imaginary; for $(\lambda - a_1)^2 < 5R$, there are two pairs of conjugate complex roots. Consider first $(\lambda - a_1)^2 > 5R$. For this case, the characteristic roots of the differential equation can be written

$$\pm i(\alpha \pm \beta)$$

where

$$\left. \begin{aligned} \alpha &= \sqrt{\frac{1}{R}} \sqrt{(\lambda - a_1) + \sqrt{5R}} \\ \beta &= \sqrt{\frac{1}{R}} \sqrt{(\lambda - a_1) - \sqrt{5R}} \end{aligned} \right\} \qquad (20)$$

The solution to the differential equation is then

$$f(\xi) = C_1 \cos(\alpha + \beta)\xi + C_2 \sin(\alpha + \beta)\xi +$$

$$C_3 \cos(\alpha - \beta)\xi + C_4 \sin(\alpha - \beta)\xi \qquad (21)$$

The value of $f(\xi)$ is now substituted into the boundary conditions given by equations (15); this substitution yields a set of homogeneous equations in the constants C_1, C_2, C_3, and C_4. The existence of a nontrivial solution requires that the determinant of the coefficients be equal to zero, or

$$\begin{vmatrix} b_1 & 0 & b_2 & 0 \\ b_1 \cos(\alpha + \beta)\frac{c}{s} & b_1 \sin(\alpha + \beta)\frac{c}{s} & b_2 \cos(\alpha - \beta)\frac{c}{s} & b_2 \sin(\alpha - \beta)\frac{c}{s} \\ 0 & b_3 & 0 & b_4 \\ -b_5 \sin(\alpha + \beta)\frac{c}{s} & b_5 \cos(\alpha + \beta)\frac{c}{s} & -b_6 \sin(\alpha - \beta)\frac{c}{s} & b_6 \cos(\alpha - \beta)\frac{c}{s} \end{vmatrix} = 0$$

where

$$b_1 = \frac{a_2}{R} - (\alpha + \beta)^2$$

$$b_2 = \frac{a_2}{R} - (\alpha - \beta)^2$$

$$b_3 = (\alpha + \beta)\left[(\alpha + \beta)^2 + \frac{a_2}{R} - \frac{4}{R}(\lambda - a_1)\right]$$

$$b_4 = (\alpha - \beta)\left[(\alpha - \beta)^2 + \frac{a_2}{R} - \frac{4}{R}(\lambda - a_1)\right]$$

$$b_5 = -(\alpha + \beta)\left[\frac{4}{R} a_3 + (\alpha + \beta)^2\right]$$

$$b_6 = -(\alpha - \beta)\left[\frac{4}{R} a_3 + (\alpha - \beta)^2\right]$$

After the determinant has been expanded and simplified, the following equation is obtained:

$$\frac{\sin^2\beta \frac{c}{s}}{\sin^2\alpha \frac{c}{s}} = \left(\frac{\beta}{\alpha}\right)^2 \left[\frac{\left(\lambda - a_1 + A_1\right)\left(\lambda - a_1 + A_2\right)}{\left(-\lambda + a_1 + A_3\right)\left(\lambda - a_1 - A_4\right)}\right] \qquad (22)$$

where

$$A_1 = \frac{1}{2}\sqrt{\frac{R}{5}\left(5 - \frac{a_2^2}{4R}\right)} - \frac{1}{2}a_2$$

$$A_2 = \frac{1}{2}\sqrt{5R}\left(1 + \frac{4a_3}{a_2}\right) + \left(a_3 - \frac{2R}{a_2}\right)$$

$$A_3 = \frac{1}{2}\sqrt{\frac{R}{5}\left(5 - \frac{a_2^2}{4R}\right)} + \frac{1}{2}a_2$$

$$A_4 = \frac{1}{2}\sqrt{5R}\left(1 + \frac{4a_3}{a_2}\right) - \left(a_3 - \frac{5R}{a_2}\right)$$

Equation (22) is valid only when $\left(\lambda - a_1\right)^2 \geqq 5R$. For values of $\left(\lambda - a_1\right)^2 < 5R$, the quantity β becomes imaginary. The corresponding divergence equation can be obtained directly from equation (22) by replacing β by $i\bar{\beta}$ where

$$\bar{\beta} = \sqrt{\frac{1}{R}}\sqrt{\sqrt{5R} - \left(\lambda - a_1\right)} \tag{23}$$

The result is

$$\frac{\sinh^2\bar{\beta}\,\frac{c}{s}}{\sin^2\alpha\,\frac{c}{s}} = \left(\frac{\bar{\beta}}{\alpha}\right)^2\left[\frac{\left(\lambda - a_1 + A_1\right)\left(\lambda - a_1 + A_2\right)}{\left(-\lambda + a_1 + A_3\right)\left(\lambda - a_1 - A_4\right)}\right] \tag{24}$$

Equation (22) (or (24)) gives an implicit relationship between the aerodynamic parameter λ and the structural parameters $(EI)_e/sD$, μ, and c/s. If $(EI)_e/sD$ and μ are fixed, then the values of A_n are known and the variation of λ with c/s can be computed by a trial-and-error process. Since c/s appears in equation (22) (or (24)) more simply than λ, this computation can be accomplished most easily by choosing values of λ and solving for the corresponding values of c/s, where they exist.

Approximate Solution

In the aeroelastic analysis of low-aspect-ratio wings of practical construction, a closed-form solution such as that described in the preceding section would not be feasible; some sort of further approximation would be necessary. One type of approximate procedure is to restrict the allowable chordwise deflection shape to a polynomial of finite degree. The present configuration (fig. 1) furnishes an excellent test for the accuracy of this procedure.

The consequences of assuming linear chordwise deflections can be obtained by allowing the chordwise stiffeners to be rigid $\left(\dfrac{(EI)_e}{sD} = \infty\right)$.

In order to obtain results for higher degrees, it is necessary to start with the energy expression (eq. (9)). Letting

$$f(x) = d_0 + d_1\left(\frac{x}{s}\right) + d_2\left(\frac{x}{s}\right)^2 + d_3\left(\frac{x}{s}\right)^3 + \ \cdot \ \cdot \ \cdot$$

then minimizing the potential energy with respect to d_1, d_2, d_3 . . ., and finally substituting the appropriate expressions for P_1 and V_1 from equations (13) yields a set of homogeneous simultaneous equations. For the cubic approximation, the equations are:

$$
\begin{bmatrix}
5 & \dfrac{5}{2}\left(\dfrac{c}{s}\right) + \dfrac{\lambda}{c/s} & B_2 + 2\lambda & B_5 + 3\lambda\,\dfrac{c}{s} \\[2ex]
\dfrac{5}{2} & B_1 & B_3 + \lambda & B_6 + 2\lambda\,\dfrac{c}{s} \\[2ex]
\dfrac{B_2}{(c/s)^2} & \dfrac{B_3}{c/s} & B_4 + \dfrac{2}{3}\lambda & B_7 + \dfrac{3}{2}\lambda\,\dfrac{c}{s} \\[2ex]
\dfrac{B_5}{(c/s)^3} & \dfrac{B_6}{(c/s)^2} & \dfrac{B_7}{c/s} + \dfrac{1}{2}\lambda & B_8 + \dfrac{6}{5}\lambda\,\dfrac{c}{3}
\end{bmatrix}
\begin{vmatrix} d_0 \\[2ex] d_1 \\[2ex] d_2 \\[2ex] d_3 \end{vmatrix}
=
\begin{vmatrix} 0 \\[2ex] 0 \\[2ex] 0 \\[2ex] 0 \end{vmatrix}
\qquad (25)
$$

where

$$B_1 = \frac{5}{3}\left[\frac{c}{s} + \frac{2(1 - \mu)}{c/s}\right]$$

$$B_2 = \frac{5}{3}\left[\left(\frac{c}{s}\right)^2 + \mu\right]$$

$$B_3 = \frac{5}{4}\left(\frac{c}{s}\right)^2 + \frac{5}{2}\left(\frac{4}{3} - \mu\right)$$

$$B_4 = \frac{R}{(c/s)^2} + \left(\frac{c}{s}\right)^2 + \frac{10}{3}\left(\frac{4}{3} - \mu\right)$$

$$B_5 = \frac{5}{4}\frac{c}{s}\left[\left(\frac{c}{s}\right)^2 + 2\mu\right]$$

$$B_6 = \left(\frac{c}{s}\right)^3 + \frac{5}{3}\frac{c}{s}(2 - \mu)$$

$$B_7 = \frac{3}{2}\frac{R}{c/s} + \frac{5}{6}\left(\frac{c}{s}\right)^3 + \frac{10}{3}\frac{c}{s}\left(\frac{3}{2} - \mu\right)$$

$$B_8 = \frac{3R}{c/s} + \frac{5}{7}\left(\frac{c}{s}\right)^3 + 4\frac{c}{s}\left(\frac{3}{2} - \mu\right)$$

The value of λ can now be found for known values of $(EI)_e/sD$, μ, and c/s by setting the determinant of equation (25) equal to zero. For the parabolic approximation, the corresponding determinant can be found by deleting the last row and column of the matrix in equation (25).

Computed results as obtained from this approximate analysis as well as those obtained from the more exact analysis are presented and discussed in the following section.

RESULTS AND DISCUSSION

The results of the exact divergence-speed calculations for a low-aspect-ratio wing for which Poisson's ratio equals 1/3 are shown in figure 2. The terms "exact" and "approximate" are used to denote exact and approximate solutions to the approximate formulation of the static aeroelastic problem presented herein. In this figure (fig. 2) the results are given in the form of a plot of the divergence-speed parameter λ against c/s for various values of the beam-to-plate stiffness ratio $(EI)_e/sD$. Results are shown only for values of c/s greater than unity because of the obvious limitations of the slender-body theory for smaller values. As is to be expected the effect of adding chordwise stiffness to the wing is to increase the divergence speed. The values of λ for $(EI)_e/sD = \infty$ (corresponding to a wing in which the chordwise bending is neglected) increase without limit as c/s becomes large (or aspect ratio becomes small). On the other hand, the values of λ for a finite $(EI)_e/sD$ apparently reach a constant value. The curves actually undulate slightly; however, the deviation from a straight line is so small that it is not apparent in the figure.

The accuracy of the linear, parabolic, and cubic approximations for the chordwise deflection shape is illustrated in figure 3. In this figure the variation of λ with c/s for the approximate solutions is compared with that for the "exact" solution for the case of zero chordwise stiffening. It can be seen that the linear approximation is unsatisfactory for all values of c/s greater than unity. The parabolic approximation gives values of λ accurate to within 10 percent of the exact value for c/s less than 2.2. The range of this accuracy is extended for the cubic approximation to c/s equal to 4.

An examination of the mode shapes at divergence is of interest. The mode shapes for $(EI)_e/sD = 0$ are shown in figure 4 for three values of c/s. These values of c/s correspond to the positions indicated by the ticks on the curve for $(EI)_e/sD = 0$ in figure 2. It can be seen that the effect of increasing c/s is essentially to extend the mode shape rearward; the shape near the leading edge changes only slightly.

Also shown in figure 4 is the mode shape for $c/s = \infty$. This shape can be obtained in the following manner:

For all the solutions obtained for finite c/s, the parameters are such that the value of β (eq. (20)) is imaginary; therefore, two of the homogeneous solutions of the differential equation (14) approach zero and two approach infinity as ξ approaches infinity. If the latter

two solutions are omitted, an equation governing divergence is obtained through the use of the boundary conditions at the leading edge only. This equation is

$$\lambda = a_1 + A_3 \tag{26}$$

which gives an asymptotic value that agrees within plottable accuracy with the flat portions of the curves in figure 2. The corresponding mode shape is

$$f(\xi) = \frac{e^{-\bar{\beta}\xi}\sin(\alpha\xi + \theta)}{\sin\theta} \tag{27}$$

where

$$\theta = \tan^{-1}\frac{2\alpha\bar{\beta}}{\dfrac{a_2}{R} - \alpha^2 + \bar{\beta}^2}$$

Note that equations (26) and (27) hold for finite values of $(EI)_e/sD$ as well as for $(EI)_e/sD = 0$. The variation of λ for large c/s with $(EI)_e/sD$ is shown in figure 5. The increase in divergence speed resulting from chordwise stiffeners is clearly evident.

CONCLUDING REMARKS

The present analysis of the static aeroelastic divergence of low-aspect-ratio rectangular wings indicates that the deflection shape in the chordwise direction has an increasing number of waves as the aspect ratio is reduced. The inclusion of additional chordwise stiffening reduces the amount of chordwise bending and, consequently, increases the divergence speed. Approximating the chordwise deflection shape by parabolic and cubic curves yields divergence speeds in fair agreement with the predictions of the more exact theory if the aspect ratio is not too

low. The cubic approximation is more accurate than the parabolic one
primarily in that configurations of lower aspect ratio can be treated
without the error becoming excessive.

Langley Aeronautical Laboratory,
    National Advisory Committee for Aeronautics,
        Langley Field, Va., January 24, 1957.

REFERENCES

1. Miles, John W.: Chordwise Divergence of Delta Wings. Rep. No. AL-1197,
    North American Aviation, Inc., Nov. 21, 1950.

2. Biot, M. A.: The Divergence of Supersonic Wings Including Chordwise
    Bending. Jour. Aero. Sci., vol. 23, no. 3, Mar. 1956, pp. 237-251.

3. Jones, Robert T.: Properties of Low-Aspect-Ratio Pointed Wings at
    Speeds Below and Above the Speed of Sound. NACA Rep. 835, 1946.
    (Supersedes NACA TN 1032.)

4. Söhngen, Heinz: Die Lösungen der Integralgleichung $g(x) = \dfrac{1}{2\pi} \oint_{-a}^{a} \dfrac{f(\xi)}{x-\xi}\, d\xi$

    und deren Anwendung in der Tragflügeltheorie. Mathematische Zs.,
    vol. 45, 1939, pp. 245-264.

5. Timoshenko, S.: Vibration Problems in Engineering. Second ed.,
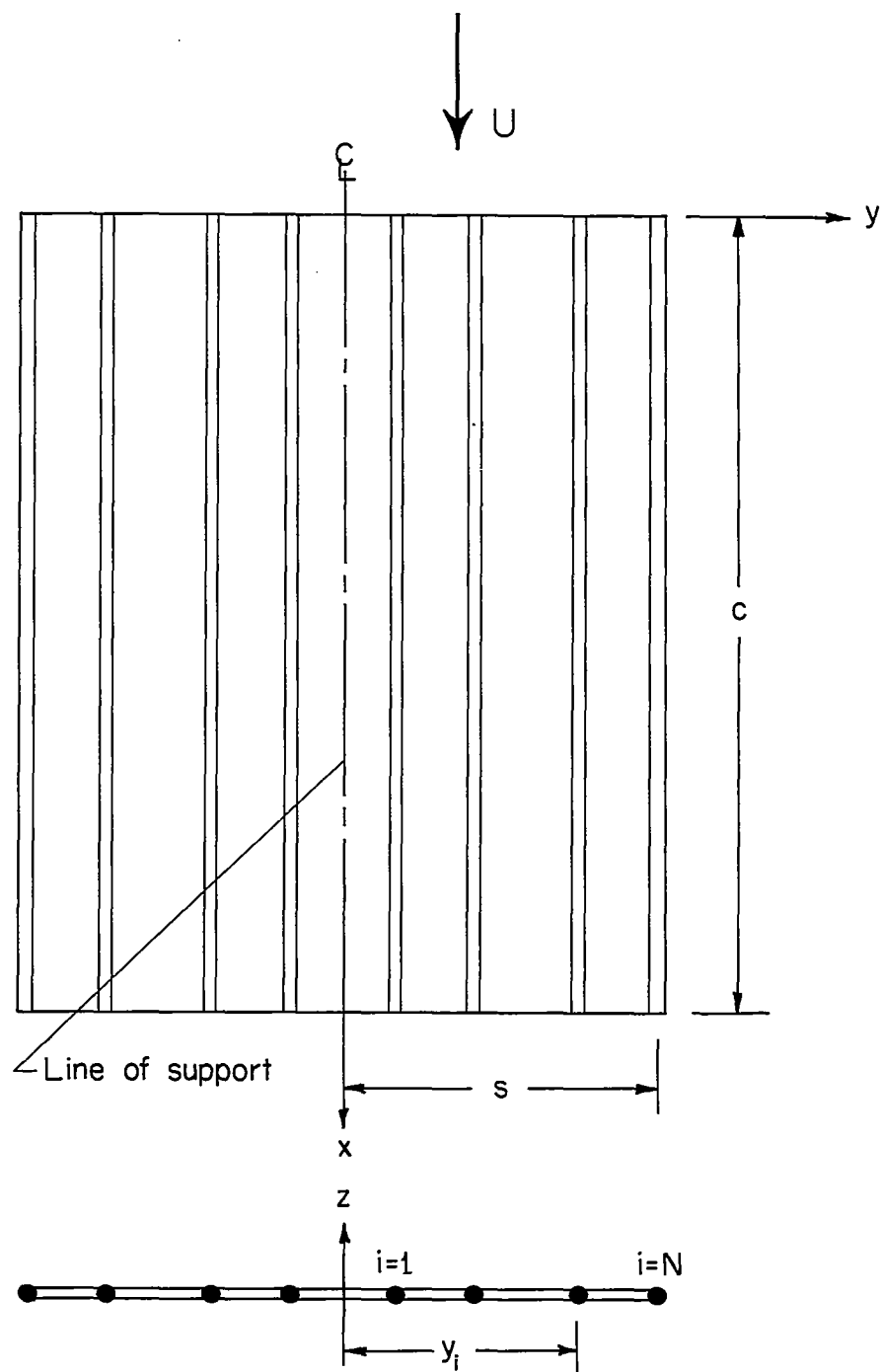   D. Van Nostrand Co., Inc., 1937, ch. VI, pp. 421-434.

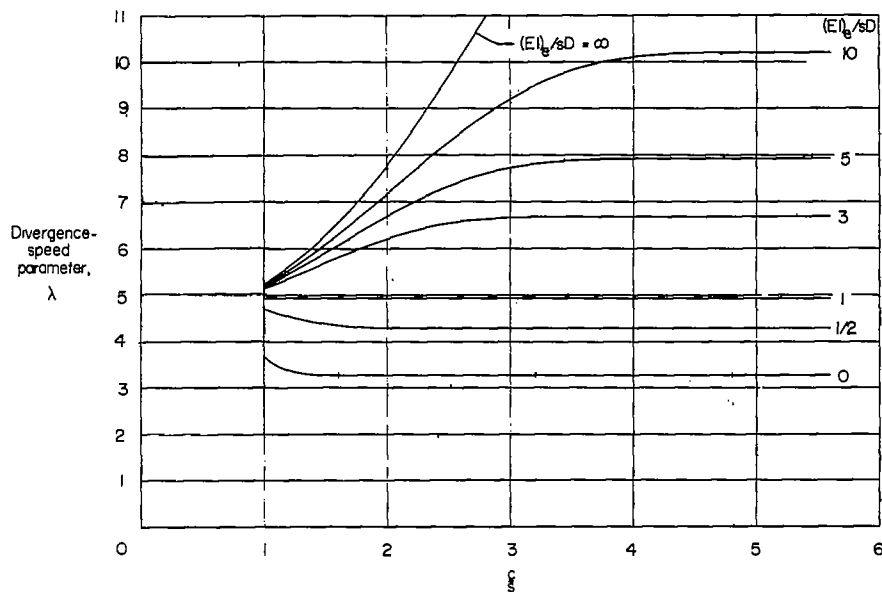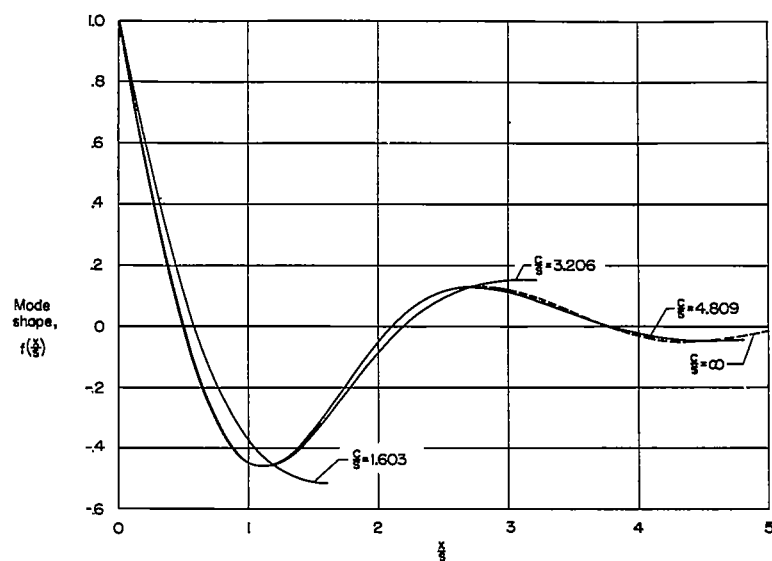Figure 1.- Configuration considered in analysis.

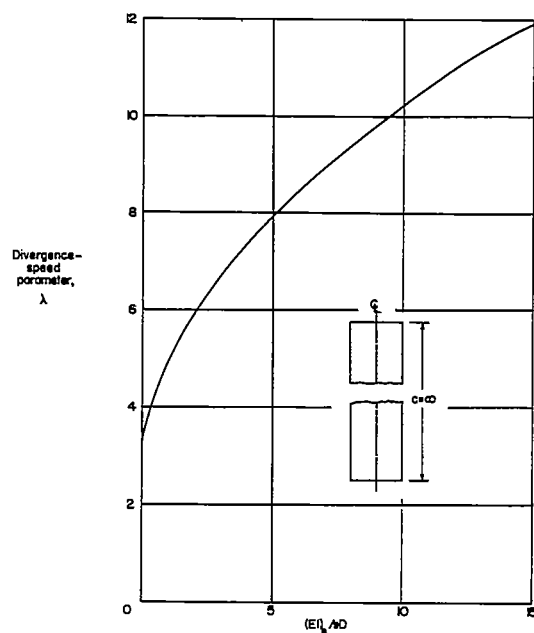Figure 4.- Chordwise variation of deflection at divergence for $(EI)_e/sD = 0.$ $\mu = 1/3.$

Figure 5.- Limiting value of divergence-speed parameter for vanishingly small aspect ratio. $\mu = 1/3.$